International Journal of Heat and Mass Transfer 58 (2013) 457–470

Contents lists available at SciVerse ScienceDirect

International Journal of Heat and Mass Transfer

journal homepage: www.elsevier.com/locate/ijhmt

Numerical study of heat transfer and blood flow in two-layered porous liver tissue during microwave ablation process using single and double slot antenna

Phadungsak Rattanadecho *, Pornthip Keangin

Research Center of Microwave Utilization in Engineering (R.C.M.E.), Department of Mechanical Engineering, Faculty of Engineering, Thammasat University (Rangsit Campus), Pathumthani 12120, Thailand

ARTICLE INFO

Article history:
Received 11 July 2012
Received in revised form 7 October 2012
Accepted 15 October 2012

Keywords:
Double slot antenna
Finite element
Liver
Microwave ablation
Porous media
Single slot antenna

ABSTRACT

Microwave ablation (MWA) is a process that uses the heat from microwave energy to kill cancer cells without damaging the surrounding tissue. MWA is emerging as an attractive modality for thermal therapy of large soft tissue targets in short periods of time, making it particularly suitable for ablation of liver cancer. The effectiveness of this technique is related to the temperature achieved during the process, as well as the input microwave power and heating time of treatment. The models of heat and blood flow transport have been used extensively in the study of MWA process and a strong tool for predicting the temperature profile, blood velocity profile and coagulation zone. These models play important role in the optimization of devices and economical way to evaluate new hypothetical designs. Furthermore, they can be used as a guideline for the practical treatment. In this work, the interstitial MWA in two-layered porous liver by single slot microwave coaxial antenna (MCA) and double slot MCA is carried out. A complete mathematical model of MWA of the porous media approach is proposed, which uses transient momentum equations (Brinkman model extended Darcy model) and energy equation coupled with electromagnetic wave propagation equation to describe the specific absorption rate (SAR) profile, temperature profile and blood velocity profile within the porous liver. The coupled nonlinear set of these equations is solved using the axisymmetric finite element method (FEM). The role of transport phenomena in two layers porous media (layers of tumor and normal tissue) for advancing the progress in biomedical applications is investigated numerically. The study aims to understand of the influences of antenna type on the SAR profile, temperature profile and blood velocity profile. In particular, the results calculated from a porous media model are compared with the results calculated from a bioheat model as well as the experimental results from previous work in order to show the validity of the numerical results. The results show that the maximum SAR, temperature and blood velocity appears within the porous liver when using a single slot MCA which is higher than when using a double slot antenna. However, the volumetric SAR, temperature and blood velocity profile within the porous liver when using a double slot MCA provides a wider region in porous liver around the slot MCA and has two hot spot zones which occurs in the vicinity of these double slots.

© 2012 Elsevier Ltd. All rights reserved.

1. Introduction

Microwave ablation (MWA) is a process that uses the heat from microwave energy to kill cancer cells. The energy from the microwave frequency waves emitted by the microwave coaxial antenna (MCA) creates heat in the local cancerous tissue cancer without the damaging surrounding tissue. The microwave energy applied to the tumor causes water molecules to vibrate and rotate, resulting in heat to a temperature high enough to cause cell death. The goal of MWA is to elevate the temperature of un-wanted tissue to 50 °C where cancer cells are destroyed [1]. MWA is a minimally invasive modality for the local treatment of solid tumors and can also enhance the effects of certain anticancer drugs [2]. Many research shows that MWA has a larger zone of active heating than Radio Frequency (RF), and its delivery does not rely on tissue texture and impedance [3,4]. Therefore, MWA is one promising alternative for cancer treatment particularly suitable for treatment of liver cancer. Several antennas have been developed for MWA within the liver, such as the slot antenna [5,6], floating sleeve antenna [7], triaxial antenna [8,9] and cooled-shaft antenna [10,11]. However, the slot antenna is extremely important for MWA application because of their small dimensions and low cost to manufacture [12]. Moreover, the heating characteristic of the slot antenna is uniform and spherical-like heating region, which is more suitable for the interstitial MWA process [13].

* Corresponding author. Tel.: +66 0 2564 3001 9; fax: +66 0 2564 3010.
E-mail address: ratphadu@engr.tu.ac.th (P. Rattanadecho).

0017-9310/$ - see front matter © 2012 Elsevier Ltd. All rights reserved.
http://dx.doi.org/10.1016/j.ijheatmasstransfer.2012.10.043

Nomenclatures

c	speed of light in free space (m/s)
C_p	specific heat capacity (J/(kg °C))
D	tumor diameter (cm)
$\vec{E}$	electric field (V/m)
f	microwave frequency (Hz)
F_0	normal stress (N/m^2)
g	gravitational constant (m^2/s)
H	magnetic field (A/m)
k	propagation constant (m^{-1})
K	thermal conductivity (W/(m °C))
p	pressure (N/m^2)
P	input microwave power (W)
Q	heat source (W/m^3)
r	dielectric radius (m)
t	time (s)
T	temperature (°C)
$\vec{u}$	velocity (m/s)
u, w	velocity component (m/s)
Z	wave impedance in the dielectric of the coaxial cable (Ω)

Greek letters

β	coefficient of the thermal expansion (1/K)
μ	magnetic permeability (H/m)
ε	permittivity (F/m)
σ	electric conductivity (S/m)
λ	wave length (m)
ω	angular frequency (rad/s)
ρ	density (kg/m^3)
ϕ	porosity (–)
ν	kinematics viscosity (m^2/s)
κ	permeability (m^2)
η	dynamic viscosity (Pa.s)

Subscripts

b	blood
eff	effective
ext	external
inner	inner
met	metabolic
n	normal tissue
outer	outer
r	relative
r, z	components of cylindrical coordinates and φ
s	solid
t	tumor
0	free space, initial condition

Superscript

T	transpose of matrix

Of many previous studies on design the slot antenna for interstitial microwave hyperthermia. Two major parameters of slot antenna are number of slot and length from tip to the center of the slot have been widely studied. The effect of two parameters on specific absorption rate (SAR) and temperature distribution were studied both theoretically and experimentally. The studied the effect of number of slot have been investigated [5,14,15]. Terakawa et al. [14] measured SAR distribution from a thin three slot antenna for microwave hyperthermia. The result shows that the high SAR was obtained around the antenna tip and the distribution was considerably tailed along the cable to the surface of the phantom. This might be caused by a reflected electric current flowing back on the outside of the cable. Many previous work carried out on the numerical simulation and experimental of interstitial for thermal ablation process in biological tissues using a double slot antenna. The clinical trials of interstitial microwave hyperthermia by used the single and array coaxial double slot antenna were presented by Saito et al. [5]. Moreover, the dependency on the insertion depth of the heating pattern around the antenna were investigated in order to confirm the treatment. Next, Rubio et al. [15] studied both numerical and experimental interstitial microwave hyperthermia by a double slot antenna using two different numerical methods, the finite element method (FEM) and a finite-difference time-domain (FDTD) method. The result shows that the numerical result using FEM corresponds very well to the experimental result in temperature distribution. The effect of the length from tip to the center of the slot on SAR distribution during microwave hyperthermia were studied [16,17]. Hyodo et al. [16] measured SAR distribution from a single slot antenna in microwave hyperthermia. The result shows that the higher length from tip to the center of the slot provides a higher SAR value than the SAR value of lower length from tip to the center of the slot. However, there are few studies on the effect of slot antenna type on the SAR and temperature distribution in the couple way.

Because of the ethical consideration, the experimental cancer therapy cannot be carried out on live human beings. Consequently, there are experimental studies in animals [18]. However, they may not represent a realistic situation of cancer treatment. Therefore, modeling of heat transport is needed in order to completely explain the actual process of MWA within the biological tissue. Numerical simulation has been widely used to study MWA as it offers a fast and economical way to evaluate new hypothetical designs. In addition, to accurately predict heating patterns within the liver and control of input microwave power and heating time during MWA process. Of many previous studies on modeling of heat transfer for MWA using a slot antenna within the biological tissue using Pennes's bioheat equation. Pennes's bioheat equation, introduced by Pennes [19] based on the heat diffusion equation. Li et al. [13] investigated microwave hyperthermia of biological tissue on heat transfer model of bioheat equation using FDTD method. The SAR distribution from coaxial slot antenna with choke is compared with the SAR distribution from monopole antenna. The result shows that the SAR pattern for monopole antenna is teardrop-like and obvious back radiation while the coaxial slot antenna with choke has the SAR distribution is more localized and more spherical-like, which is more suitable for the interstitial microwave hyperthermia. Due to simplifications and many assumptions of bioheat model, other workers have established mathematical bioheat models by extending or modifying Pennes model. The study of high temperatures tissue ablation using a modified bioheat equation to include tissue internal water evaporation during heating has been proposed [20]. The simulation result of modified bioheat equation is found in agreement well to the experimental result.

Some research group used the coupled model of Pennes's bioheat equation and others model for analyzed the temperature increase in biological tissue, such as Özen et al. [21] analyzed the temperature increase in one dimensional three-layers skin tissue model exposed to microwaves by using finite difference method.

The results calculated from a thermal wave model of bioheat transfer (TWMBT) are compared with the results calculated from a Pennes's bioheat equation, it was found that the temperature increase in skin of TWMBT lower than the Pennes's bioheat equation. After that Keangin et al. [22] carried out on the numerical simulation of liver cancer treated using the mathematical model considered the coupled model of electromagnetic wave propagation and bioheat transfer.

In realistic, the biological tissue including cell and microvascular bed with the blood flow direction contains many vessels and can be regarded as a porous structure. Thus, the study of heat transport in biological tissue should used porous media theory. Description of the established porous media models can be found in the literature [23]. Nevertheless, most of the works have concentrated on only the heat transport model however do not consider electromagnetic wave propagation model. Moreover, most concentrated on single-layer porous media biomaterials. Nakayama and Kuwahara [24] derived a general set of bioheat transfer equations for blood flows and its surrounding biological tissue using a two-energy equation model. Mahjoob and Vafai [25] analyzed characterization of heat transport through biological media incorporating hyperthermia treatment, utilizing the local thermal non-equilibrium model of porous media theory, exact solutions for the tissue and blood temperature profiles have been established. They considered the effect of parameters such as the vascular volume fraction, tissue permeability, blood flow rate, metabolic heat generation and body core temperature on blood and tissue phase temperature profiles. Afrin et al. [26] presented a generalized dual-phase lag mode for living biological tissues based on nonequilibrium heat transfer between tissue, arterial and venous bloods. Their work studied the effect of thermo physical properties of blood and surrounding tissue on phase lag times for heat flux and temperature gradient in brain and muscles. The results showed that the phase lag times for heat flux and temperature gradient are the identical for the case that the tissue and blood have the same properties. A few studies considered model of heat transport of layered biomaterials and concentrated the complete mathematical model considered the coupled model of electromagnetic wave propagation, heat transfer and blood flow, especially a detailed study of the effect of antenna type on the SAR, temperature and flow patterns. This is because complexity of the dielectric and thermal properties in each layer as affected by the SAR, temperature and blood velocity profile within the layered materials. The complete mathematical model is useful for the development of biomedical technologies especially.

In this study, the influence of antenna type namely single slot microwave coaxial antenna (MCA) and double slot MCA on SAR, temperature and blood velocity profile within the porous liver during MWA process have been investigated. This work is substantially extended from our previous work [22] in which the formulated model based on porous media approach in two layers liver is proposed. Mathematical model of the process involved in MWA are based on transient momentum equations (Brinkman model extended Darcy model) and energy equation coupled with electromagnetic wave propagation equation. The coupled nonlinear set of governing equations as well as initial and boundary conditions are solved using the axisymmetric FEM via COMSOL™ Multiphysics. In order to verify the accuracy of the presented mathematical model of MWA, the resulting data is validated against the experimental results, obtained by Yang et al. [20]. The comparison of the result calculated from porous media model with the bioheat model in our previous studies [22] is also considered in order to test the efficiency of the proposed model. The results of distribution of SAR, temperature and blood velocity are presented in details. The analysis from this study serves as essential fundament for the development of mathematic models of heat transfer and blood flow phenomena and can be used as a guideline for the practical treatment.

2. Problem statement

Slot coaxial antennas are the most popular antennas in MWA application of the advantages, its size (small dimensions), design simplicity, low cost to manufacture and convenient adaptation to treatment. This study uses a single slot MCA and double slot MCA, to transfer microwave power into the porous liver for the treatment of liver cancer. The antennas are composed of a thin semi-rigid coaxial cable. Since the antennas are intended to be inserted into the human body, it is desirable that the outer diameter be as small as possible. These antennas have a diameter of 1.79 mm because the thin antenna is required in the interstitial treatments. A ring-shaped slot, 1 mm wide is cut off the outer conductor 5.5 mm in length from the short circuited tip of the antenna to allow electromagnetic wave propagation into the tissue because the effective heating around the tip of the antenna is very important to the interstitial heating and because the electric field becomes stronger near the slot [27]. Our design uses a 1 mm wide in each slot, which is easily fabricated, and also gives minimal power reflection [28]. The antennas are composed of an inner conductor, a dielectric and an outer conductor. The antennas are enclosed in a catheter (made of polytetrafluorethylene; PTFE), for hygienic to prevent adhesion of the probe to desiccated ablated tissue and guidance purposes. Fig. 1(a) and (b) shows the model geometry of a single slot MCA and a double slot MCA, respectively. The antennas are operated at the frequency of 2.45 GHz, a widely used frequency in MWA and is one of the ISM (Industrial, Scientific, and Medical) dedicated frequencies. In case of double slot MCA, the slot spacing is chosen based on the effective wavelength (λ_{eff}) in tissue at frequency of 2.45 GHz, which is calculated using the following equation [29]:

$$\lambda_{eff} = \frac{c}{f\sqrt{\varepsilon_r}} \tag{1}$$

where c is the speed of light in free space (m/s), f is the operating frequency of the microwave generator (2.45 GHz) and ε_r is the relative permittivity of tissue at the operating frequency.

For the double slot MCA, the slot spacing length of 4.2 mm corresponds to 0.25 λ_{eff}. The slot spacing length is chosen to achieve localized power deposition near the distal tip of the antenna. Dimensions of antennas are given in Table 1. While the dielectric properties of antennas are given in Table 2.

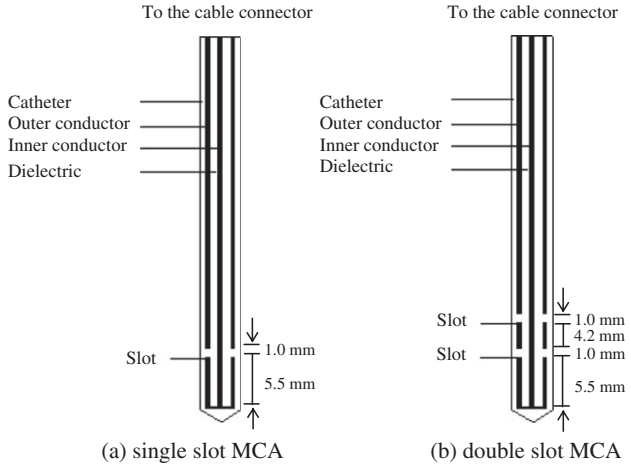

Fig. 1. Model geometry of a MCA (a) single slot MCA (b) double slot MCA.

Table 1
Dimensions of a MCA.

Materials	Dimensions (mm)
Inner conductor	0.135 (radial)
Dielectric	0.335 (radial)
Outer conductor	0.460 (radial)
Catheter	0.895 (radial)
Slot	1.000 (wide)

Table 2
The dielectric properties of a MCA.

Properties	Relative permittivity ε_r	Electric conductivity σ (S/m)	Relative permeability μ_r
Dielectric	2.03	0	1
Catheter	2.1	0	1
Slot	1	0	1

The porous liver consists of two parts, namely, the normal tissue and the tumor. The porous liver is considered as a cylindrical geometry, it has a 30 mm radius and 80 mm in height. Within the porous liver there is a spherical tumor with diameter of 20 mm. The antennas are inserted into the porous liver with 70.5 mm depth. An axially symmetric model is considered in this study, which minimized the computation time while maintaining good resolution and represents the full three-dimensional result. The model assumes that the antennas are immersed in a porous biological tissue. The vertical axis is oriented along the longitudinal axis of the antennas, and the horizontal axis is oriented along the radial direction. Figs. 2(a) and 2(b) show the axially symmetrical model geometry for analysis when using a single slot MCA and a double slot MCA, respectively.

In an anatomical view, three compartments are identified in the biological tissues, namely, blood vessels, cells and interstitial space [24,25]. The interstitial space can be further divided into the extracellular matrix and the interstitial fluid. However, for sake of simplicity, the biological tissues are divided into two distinctive regions, namely, the vascular region (blood vessels) and the extra-vascular region (cells and the interstitial space) and treat the whole anatomical structure as a fluid-saturated porous medium, through which the blood infiltrates. The vascular region is regarded as a blood phase and extra-vascular region is regarded as a solid phase, as illustrated in Fig. 2.

The physical properties of the materials involved in the model are selected from several literatures; [20,28,30–32]. The thermal properties and dielectric properties of normal tissue, blood and tumor used for mathematical calculations are given in Table 3 where the microwave frequency of 2.45 GHz is considered.

3. The formulation of the mathematical model

A mathematical model has been formulated to predict the SAR profile, temperature profile and blood velocity profile in the porous liver during the MWA process. In the next section, an analysis of electromagnetic wave propagation, blood flow and heat transfer

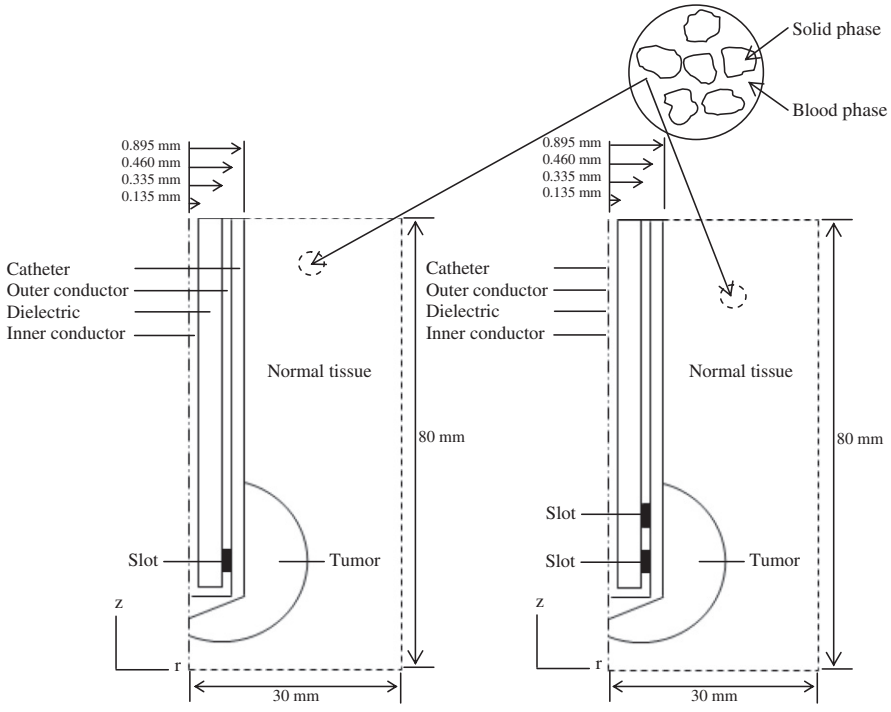

Fig. 2. Axially symmetrical model geometry.

Table 3
The thermal properties and dielectric properties of normal tissue, blood and tumor [20,28,30–32].

Properties	Thermal conductivity K (W/m °C)	Density ρ (kg/m^3)	Specific heat capacity C_p (J/kg °C)	Relative permittivity ε_r	Electric conductivity σ (S/m)
Normal tissue (n)	0.497	1030	3600	43.00	1.69
Blood (b)	0.45	1058	3960	58.30	2.54
Tumor (t)	0.57	1040	3960	48.16	2.096

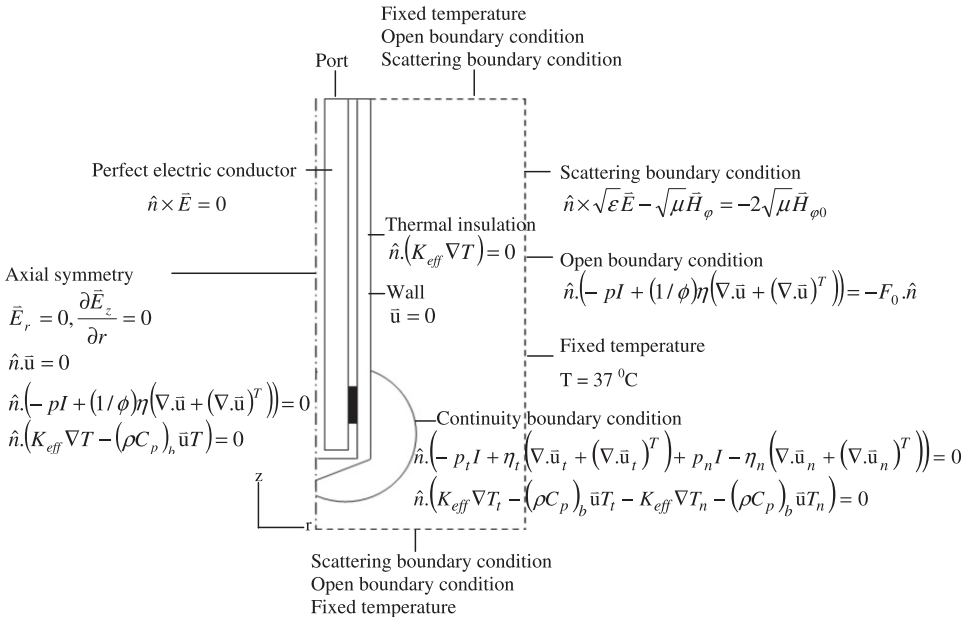

Fig. 3. Boundary conditions for analysis.

in the porous liver during MWA process will be illustrated. The system of governing equations as well as initial and boundary conditions are solved numerically using the FEM via COMSOL™ Multiphysics. The relevant boundary conditions are described in Fig. 3.

3.1. Analysis of electromagnetic wave propagation

Mathematical models are developed to predict the SAR profile with relation to temperature gradient within the porous liver. To simplify the problem, the following assumptions are made:

1. Electromagnetic wave propagation is modeled in 2D axially symmetrical cylindrical coordinates (r–z).
2. An electromagnetic wave, propagating in a MCA, is characterized by transverse electromagnetic fields (TEM) [28].
3. In the porous liver, an electromagnetic wave is characterized by transverse magnetic fields (TM) [28].
4. The model assumes that the wall of the MCA is a perfect electric conductor (PEC),
5. The outer surface of the porous liver is truncated by a scattering boundary condition.
6. The model assumes that dielectric properties of the porous liver are uniform and constant.

The axisymetric finite element (FE) model used in this study is adapted from a MCA general model [8,33]. In this model, the electric and magnetic fields associated with the time-varying TEM wave is expressed in 2D axially symmetrical cylindrical coordinates:

Electric field ($\vec{E}$)

$$\vec{E}=e_r\frac{C}{r}e^{j(\omega t-kz)} \tag{2}$$

Magnetic field ($\vec{H}$)

$$\vec{H}=e_\varphi\frac{C}{rZ}e^{j(\omega t-kz)} \tag{3}$$

where $C=\sqrt{\frac{ZP}{\pi.\ln(r_{outer}/r_{inner})}}$, Z is the wave impedance (Ω), P is the input microwave power (W), r_{inner} is the dielectric inner radius (m), r_{outer} is the dielectric outer radius (m), $\omega=2\pi f$ is the angular frequency (rad/s), f is the frequency (Hz), $k=\frac{2\pi}{\lambda}$ is the propagation constant (m^{-1}) and λ is the wave length (m).

In the porous liver, the electric field also has a finite axial component, whereas the magnetic field is purely in the azimuth direction. The electric field is in the radial direction only inside the coaxial cable and in both radial and the axial direction inside the tissue. This allows for the MCA to be modeled using an axisymmetric TM wave formulation. The wave equation then becomes scalar in $\vec{H}_\varphi$:

$$\nabla\times\left(\left(\varepsilon_r-\frac{j\sigma}{\omega\varepsilon_0}\right)^{-1}\nabla\times\vec{H}_\varphi\right)-\mu_rk_0^2\vec{H}_\varphi=0 \tag{4}$$

where $\varepsilon_0=8.8542\times10^{-12}$ F/m is the permittivity of free space, ε_r is the relative permittivity, σ is the electric conductivity (S/m), μ_r is the relative permeability and k_0 is the free space wave number (m^{-1}).

3.1.1. Boundary condition for electromagnetic wave propagation analysis

Microwave energy is emitted from the MCA slot, which connected to the microwave generator, and propagates through the MCA into the porous liver from the MCA slot. Therefore, boundary condition for analyzing electromagnetic wave propagation, as shown in Fig. 3, is considered as follows:

At the inlet of the MCA, TM wave propagation with input microwave power of 10 W is considered. An axial symmetry boundary is applied at $r=0$:

$$\vec{E}_r=0 \tag{5}$$

$$\frac{\partial\vec{E}_z}{\partial r}=0 \tag{6}$$

The first order scattering boundary conditions for $\vec{H}_\varphi$ were used along the outer sides of the porous liver boundaries to prevent reflection artifacts:

$$\hat{n}\times\sqrt{\varepsilon}\vec{E}-\sqrt{\mu}\vec{H}_\varphi=-2\sqrt{\mu}\vec{H}_{\varphi0} \tag{7}$$

where $\vec{H}_{\varphi0}=C/Zr$ is the excitation magnetic field.

For simplicity and to eliminate numerical error, the inner and outer conductors of the MCA are modeled as the PEC boundary conditions:

$$\hat{n} \times \vec{E} = 0 \tag{8}$$

3.2. Analysis of blood flow and heat transfer

To solve the thermal problem, the coupled effects of electromagnetic wave propagation, blood flow and heat transfer are investigated. The surroundings of the porous media model are fixed temperature at 37 °C except at the outer surface between the MCA and the porous liver is considered as adiabatic boundary condition. To reduce complexity of the problem, several assumptions have been offered into the blood flow and energy equations:

1. Corresponding to electromagnetic wave propagation analysis, blood flow and heat transfer analysis in the porous liver is assumed in 2D axially symmetrical cylindrical coordinates (r–z).
2. The porous liver is assumed to be homogeneous and thermally isotropic and saturated with a fluid (blood).
3. The blood flow is an incompressible and Newtonian [24,34].
4. There is local thermodynamic equilibrium (LTE) between solid and blood phases [35,36].
5. There is no phase change occurs within the porous liver, no energy exchange through the outer surface of the porous liver, and no chemical reactions occur within the porous liver.
6. The thermal properties of the porous liver are assumed to be constant.

3.2.1. Momentum equations

The Brinkman model extended Darcy model was first developed by Brinkman [37] and used to represent the blood flow within the porous liver. Using standard symbols, the governing equations describing the heat transfer phenomenon are given as follows [38]:

Continuity equation

$$\frac{\partial u}{\partial r} + \frac{\partial w}{\partial z} = 0 \tag{9}$$

Momentum equations

$$\frac{1}{\phi}\left(\frac{\partial u}{\partial t}\right) + \frac{1}{\phi^2}\left(u\frac{\partial u}{\partial r} + w\frac{\partial u}{\partial z}\right) = -\frac{1}{\rho_b}\left(\frac{\partial p}{\partial r}\right) + \frac{v}{\phi}\left(\frac{\partial^2 u}{\partial r^2} + \frac{\partial^2 u}{\partial z^2}\right) - \frac{uv}{\kappa} \tag{10a}$$

$$\frac{1}{\phi}\left(\frac{\partial w}{\partial t}\right) + \frac{1}{\phi^2}\left(u\frac{\partial w}{\partial r} + w\frac{\partial w}{\partial z}\right) = -\frac{1}{\rho_b}\left(\frac{\partial p}{\partial z}\right) + \frac{v}{\phi}\left(\frac{\partial^2 w}{\partial r^2} + \frac{\partial^2 w}{\partial z^2}\right) - \frac{wv}{\kappa} + g\beta(T - T_\infty) \tag{10b}$$

where u and w are the blood velocity component (m/s), ϕ is the tissue porosity (the volume fraction of the vascular space) (-) [24] in this study used $\phi_n = 0.6$ and $\phi_t = 0.7$, p is the pressure (Pa), $v = 3.78 \times 10^{-7}$ m^2/s is the kinematics viscosity, $\beta = 1 \times 10^{-4}$ 1/K is the coefficient of the thermal expansion and κ is the permeability (m^2) can be expressed by the following [39,40]:

$$\kappa = \frac{\phi^3 d_p^2}{175(1-\phi)^2} \tag{11}$$

where $d_p = 1 \times 10^{-4}$ m^2 is the diameter of cell tissue.

The first viscous term on the right hand side of Eq. (10) is the Darcy term while the second viscous term is the analogous to the momentum diffusion term in the Navier–Stokes equation.

Although the viscous boundary layer in the porous medium is very thin for most engineering applications, inclusion of this term is essential for heat transfer calculations [41]. However, the inertial effect was neglected, as the flow was relatively low.

3.2.2. Energy equation

The temperature profile in the porous liver during MWA process is obtained by solving the conventional heat transport equation where the microwave power absorbed is included as an internal heat sources (namely metabolic heat source). The temperature profile corresponds to the SAR. This is because when microwave propagates in the porous liver, microwave energy is absorbed as well as SAR by the porous liver and converted into internal heat generation which causes the porous liver temperature to rise. The governing equations describing the heat transfer phenomenon are given by

$$(\rho C_p)_{eff}\frac{\partial T}{\partial t} + (\rho C_p)_b\left(u\frac{\partial T}{\partial r} + w\frac{\partial T}{\partial z}\right) = K_{eff}\left(\frac{\partial^2 T}{\partial r^2} + \frac{\partial^2 T}{\partial z^2}\right) + Q_{met} + Q_{ext} \tag{12}$$

where

$$(\rho C_p)_{eff} = (1-\phi)(\rho C_p)_s + \phi(\rho C_p)_b \tag{13}$$

$$K_{eff} = (1-\phi)K_s + \phi K_b \tag{14}$$

are the overall heat capacity per unit volume and overall thermal conductivity, subscripts *eff*, *s* and *b* represent the effective value, solid and blood phase, respectively, T is the temperature (°C), ρ is the density (kg/m^3), C_p is the specific heat capacity (J/kg °C) and K is the thermal conductivity (W/m °C).

Where the first and the second terms on the left hand side of Eq. 12 denotes the transient term and convection term due to blood perfusion, respectively. The first, second and third terms on the right hand side of Eq. 12 denote the heat conduction term, metabolic heat source (Q_{met} = 33,800 W/m^3) term and external heat source (Q_{ext}) (heat generation by the electric field) term, respectively. The external heat source term is equal to the resistive heat generated by the electromagnetic field and assume only generated from solid phase which can be defined as:

$$Q_{ext} = \frac{\sigma|\vec{E}|^2}{2} \tag{15}$$

where, the electrical properties strongly affect the temperature increase. Interaction of electromagnetic fields with biological tissues can be defined in term of SAR. When microwave propagates in the porous liver, microwave energy is absorbed by the porous liver and converted into internal heat generation which causes the porous liver temperature to rise. The SAR profile is widely used to discuss the heating characteristics of MWA process. The SAR represents the electromagnetic power deposited per unit mass in tissue (W/kg) at any position. It can define by:

$$\mathrm{SAR} = \frac{\sigma|\vec{E}|^2}{2\rho} = \frac{Q_{ext}}{\rho} \tag{16}$$

3.2.3. Boundary condition for blood flow and heat transfer analysis

The blood flow and heat transfer analysis are considered only in the porous liver, which does not include the MCA. As shown in Fig. 3, the boundaries of porous liver corresponds to the assumption are considered as follows:

An axial symmetry boundary is applied at $r = 0$ for the blood flow and heat transfer analysis:

$$\hat{n} \cdot \vec{u} = 0 \tag{17}$$

$$\hat{n} \cdot \left(-pI + (1/\phi)\eta \left(\nabla \cdot \vec{u} + \left(\nabla \vec{u} \right)^T \right) \right) = 0 \tag{18}$$

$$\hat{n} \cdot \left(K_{eff} \nabla T - (\rho C_p)_b \vec{u} T \right) = 0 \tag{19}$$

The surroundings of the porous liver are fixed temperature at 37 °C and the boundaries for blood flow analysis are considered an open boundary condition:

$$\hat{n} \cdot \left(-pI + (1/\phi)\eta \left(\nabla \cdot \vec{u} + \left(\nabla \vec{u} \right)^T \right) \right) = -F_0 . \hat{n} \tag{20}$$

where η is the dynamic viscosity (Pa s) and F_0 is the normal stress (N/m^2)

At the outer surface between the MCA and the porous liver is considered as adiabatic boundary condition.

$$\hat{n} . (K_{eff} \nabla T) = 0 \tag{21}$$

Furthermore, the outer surface of MCA between the MCA and the porous liver is rigid body, a no slip boundary conditions are applied for the momentum equations.

$$\vec{u} = 0 \tag{22}$$

It is assumed that no contact resistant occurs between the normal tissue and the tumor. Therefore, the internal boundary is assumed to be a continuous.

$$\hat{n} . \left(-p_t I + \eta_t \left(\nabla . \vec{u}_t + \left(\nabla . \vec{u}_t \right)^T \right) + p_n I - \eta_n \left(\nabla . \vec{u}_n + \left(\nabla . \vec{u}_n \right)^T \right) \right) = 0 \tag{23}$$

$$\hat{n} . \left(K_{eff} \nabla T_t - (\rho C_p)_b \vec{u} T_t - K_{eff} \nabla T_n - (\rho C_p)_b \vec{u} T_n \right) = 0 \tag{24}$$

The initial temperature of the porous liver is assumed to be uniform:

$$T(t_0) = 37^{\circ}\mathrm{C} \tag{25}$$

And initial condition for the blood velocity and pressure are

$$u(t_0) = 0 \text{ m/s}, \quad w(t_0) = 0 \text{ m/s} \quad \text{and} \quad p(t_0) = 0 \text{ Pa} \tag{26}$$

4. Calculation procedure

In this study, the FEM is used to analyze the transient problems. The computational scheme is to assemble axisymmetric FEM model. The coupled model of electromagnetic wave propagation, blood flow and heat transfer analysis is solved by the FEM, to demonstrate the phenomenon that occurs within the porous liver during MWA. The computational scheme starts with computing an external heat source term by running an electromagnetic wave propagation calculation and subsequently solves the time dependent temperature and blood velocity in the porous liver. All the steps are repeated until the required heating time is reached.

The description of blood flow and heat transfer pattern, Eq. (9), (10a), (10b), (11)–(14) requires specification of temperature (T), velocities components (u,w) and pressure (p). These equations are coupled to the electromagnetic wave propagation equations (Eq. (2)–(8)) and momentum equations and energy equation by Eq. 15. The time-steps used to solve the system of equations describing electromagnetic wave propagation and heat transport are $\Delta t = 2 \times 10^{-12}$ s and $\Delta t = 0.01$ s, respectively.

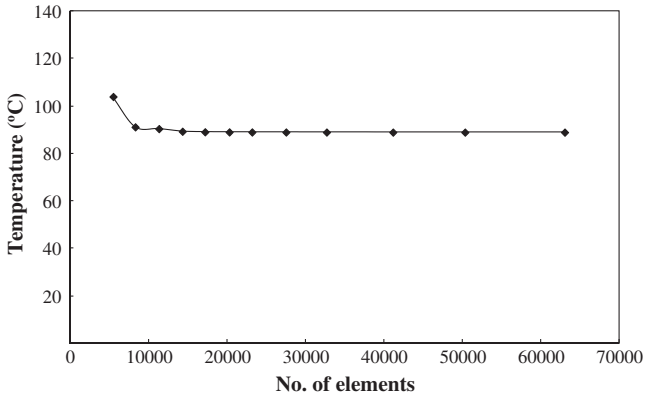

Fig. 4. Grid convergence curve of the model.

The axisymmetric FEM model is discretized using triangular elements with the Lagrange quadratic shape functions. In order to obtain a good approximation, a fine mesh is specified in the sensitive areas. The set of partial differential equations along with their related boundary conditions are coupled and are solved numerically by the FEM via COMSOL™ multiphysics. FEM models can provide users with quick, accurate solutions to multiple systems of differential equations and as such, are well suited to heat transfer problems like ablation [28]. The system of governing equations as well as initial and boundary conditions are solved with the Unsymmetric Multifrontal Method (UMFPACK) solver to approximate SAR profile, temperature profile and blood velocity profile variation across each element. The convergence test is carried out to identify the suitable numbers of element required. The convergence curve resulting from the convergence test is shown in Fig. 4. This figure shows the relationship between temperature and number of elements from simulations at a critically sensitive point, of the slot center (insertion depth of 64 mm). The number of elements where solution is independent of mesh density is found to be around 20,471. It is reasonable to confirm that, at this number of element, the accuracy of the simulation results is independent from the number of elements through the calculation process. Dense mesh zone has been generated in the vicinity of the tip of the antenna, where the temperature is more concentrated

5. Results and discussion

A complete set of mathematical model is proposed, which uses comprehensive transient momentum equations (Brinkman model extended Darcy model) and energy equation coupled with the electromagnetic wave propagation equation to describe SAR profile, temperature profile and blood velocity profile in the porous liver of MWA. The influences of antenna type on the SAR profile, temperature profile and blood velocity profile of porous liver are systematically investigated.

5.1. Validation of the model

In order to verify the accuracy of the presented mathematical model of MWA, the simulation results with single slot MCA of the single-layer porous media proposed in this study is validated against the simulation results of bioheat model obtained at the same testing condition by Keangin et al. [22]. Moreover, the simulation results from this study also compared with the experimental results obtained by Yang et al. [20]. Fig. 5 shows the geometry of the validation model. In the validation model, the input microwave

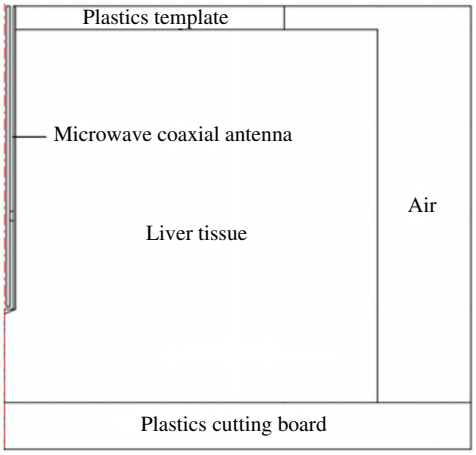

Fig. 5. Geometry of the validation model obtained from the Yang et al. [20].

power of 75 W with frequency of 2.45 GHz and the initial liver tissue temperature of 8 °C are selected. The single slot MCA with a radius of 1.25 mm is inserted into liver tissues 20 mm in depth. The axially symmetrical model is used to analyze the MWA process with the heating time of 50 s. The validation results of the selected test case are illustrated in Fig. 6 for temperature distribution in the liver tissue, with respect to the heating time of 50 s with the positions of 4.5 and 9.5 mm away from the MCA. From the figures, it can be observed that the simulated results of the porous media model corresponds well to the experimental results with similar trends in temperature distribution over the same approximate time range at both positions, especially at the end stage. This is due to the fact that the porous media model is based on convective heat mode coupled with conduction heat mode. While the bioheat model is manly governed by conduction heat mode. Considering the fact that the convective heat is influence increases at the end stage, it is obvious that the porous media model yields better results. Table 4 shows the comparisons of the root mean square error (RMSE) of the liver tissue temperature between the present study (porous media model) and our previous work [22] (bioheat model) with experimental data obtained from Yang et al. [20]. From the table, it is observed that the bioheat model gives greater error than the simulated temperature obtained from porous media model.

Table 4
Comparisons of RMSE of the liver tissue temperature between the present study and Yang et al. [20] and Keangin et al. [22].

Position (mm)	Comparisons of RMSE with experimental data obtained from Yang et al. [20] (°C)	
	Bioheat model (Keangin et al. [22])	Porous media model (present study)
4.5 mm	11.10	3.87
9.5 mm	4.52	2.73

However, at the position of 9.5 mm away from the MCA, the temperature distribution match the experimental results better than the temperature distribution at the position of 4.5 mm. Therefore, the selected developed model based on porous media approach is reasonable and can be used effectively for this problem. This is important to obtain the approaching realistic tissues modeling during MWA. It is found that the previous study [22] considered only the heat transfer in the single-layer biological tissue using the bioheat model however, in practical applications of MWA process, most biological tissues are multilayer porous materials. In addition, the antenna type has a significant effect on SAR, temperature and blood velocity profiles. Consequently, the model of MWA based on two layers porous liver model using a single and a double slot MCA for study the effect of antenna type on SAR, temperature and blood velocity profiles, is developed in this work.

5.2. Comparison of single slot MCA and double slot MCA

5.2.1. SAR profiles

The basic principle of MWA is to apply microwave power to the tumor through the MCA. The microwave energy is absorbed within the tumor and heated it. At temperatures exceeding 50 °C, tumor is destroyed [1]. The SAR profile is one of the most important characteristics of antenna for heating. Fig. 8 shows the computer simulated results of SAR profile in the porous liver based on a frequency of 2.45 GHz, input microwave power of 10 W and heating times of 300 s during MWA process. Fig. 8(a) shows the SAR profile within the porous liver when using a single slot MCA and Fig. 8(b) when using a double slot MCA for heating times of 30, 150, and 300 s, respectively. The figure illustrates the volume heating effect expected from MWA. Microwaves power emitted from

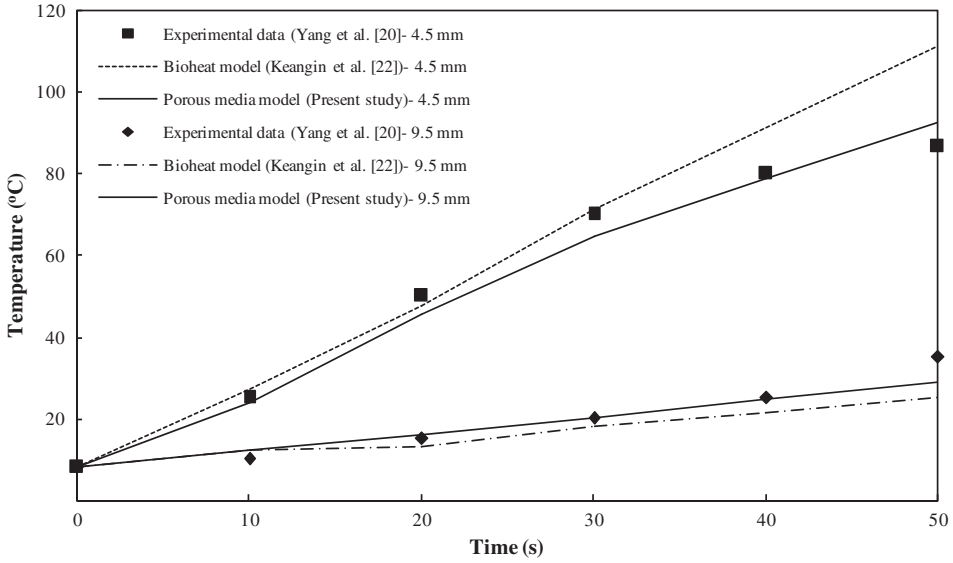

Fig. 6. The validation results of the liver tissue temperature, against Yang et al. [20] and Keangin et al. [22].

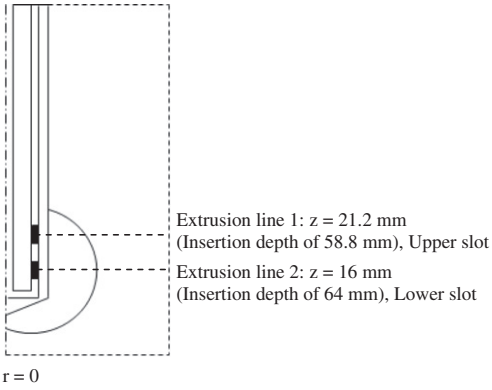

Fig. 7. The extrusion line in the porous liver where the SAR, temperature and blood velocity distribution are considered.

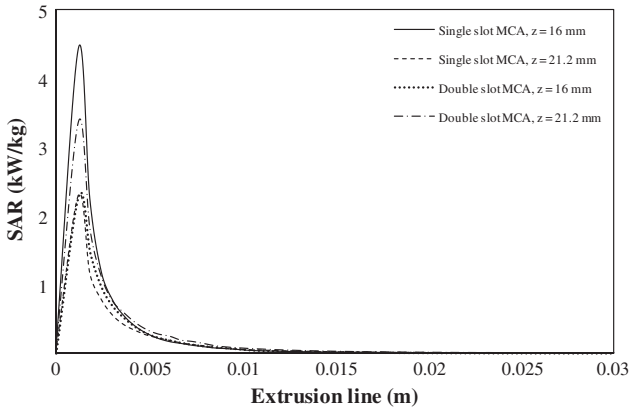

Fig. 9. Comparison of SAR distribution between when using a single slot MCA and a double slot MCA along the extrusion line.

the MCA propagates through the tumor and the normal tissue, which is converted to heat by dielectric heating. According to the results, in both cases, the SAR profile exhibits a near ellipsoidal shape around the slot. It has the highest value in the vicinity of the slot MCA and decreases with the distance lead to the SAR value within the tumor is higher than the SAR value within the normal tissue. The comparison of the SAR profile pattern between when using a single slot MCA and using a double slot MCA, it is found that the volumetric SAR within the porous liver of double slot MCA provides the two hot spot zones with a wider region of SAR pattern to the porous liver around the slot MCA. This is because of the double slot MCA have supplied microwave energy via its slot separately. Consequently the volumetric SAR in this case is seemed to be a wider region as compared to single slot MCA. The means that the single slot MCA is generally suitable for the narrow tumor. While, the double slot MCA is suitable for the larger tumor size or adjacent tumors.

Consider the maximum SAR value within the porous liver from two antennas, a standard single slot MCA provides a higher maximum SAR value within the porous liver than when using a double slot MCA. It is found that at the heating time of 300 s and using an input microwave power of 10 W, the maximum SAR values are 6.104×10^3 W/m^3 and 3.906×10^3 W/m^3 when using a single slot MCA and double slot MCA, respectively. However, in two cases, the maximum SAR values appeared near the antennas tip and the lower slot exit of the MCA.

Fig. 9 shows the comparison of SAR distribution between when using a single slot MCA and double slot MCA along the extrusion line defined in Fig. 7 at level of the upper slot exit ($z = 21.2$ mm, insertion depth of 58.8 mm) and the lower slot exit ($z = 16$ mm, insertion depth of 64 mm) based on a frequency of 2.45 GHz, input microwave power of 10 W and heating times of 300 s. From the Fig. 9, it is found that in all cases the SAR distributions have a similar trend with a slight difference in magnitude. The SAR distributions gradually increase along the longitudinal axis of the MCA and reach maximum value at the slot exit. After that the SAR values quickly decreases and have the lowest value with $r = 30$ mm. When using a single slot MCA, the maximum SAR values obtained for 10 W of input microwave power is 4.43 kW/kg and 2.30 kW/kg at

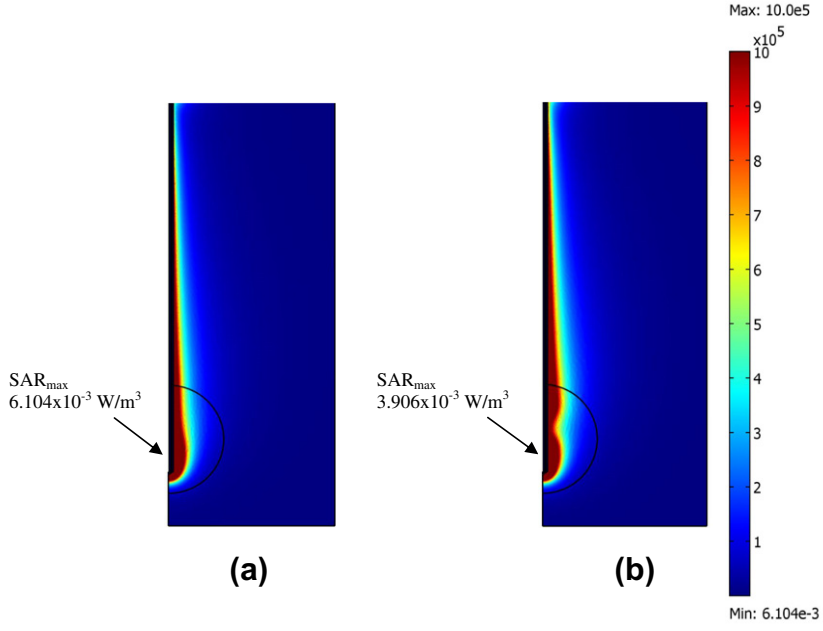

Fig. 8. The SAR profile in the porous liver based on a frequency of 2.45 GHz, input microwave power of 10 W and heating times of 300 s when using; (a) single slot MCA (b) double slot MCA.

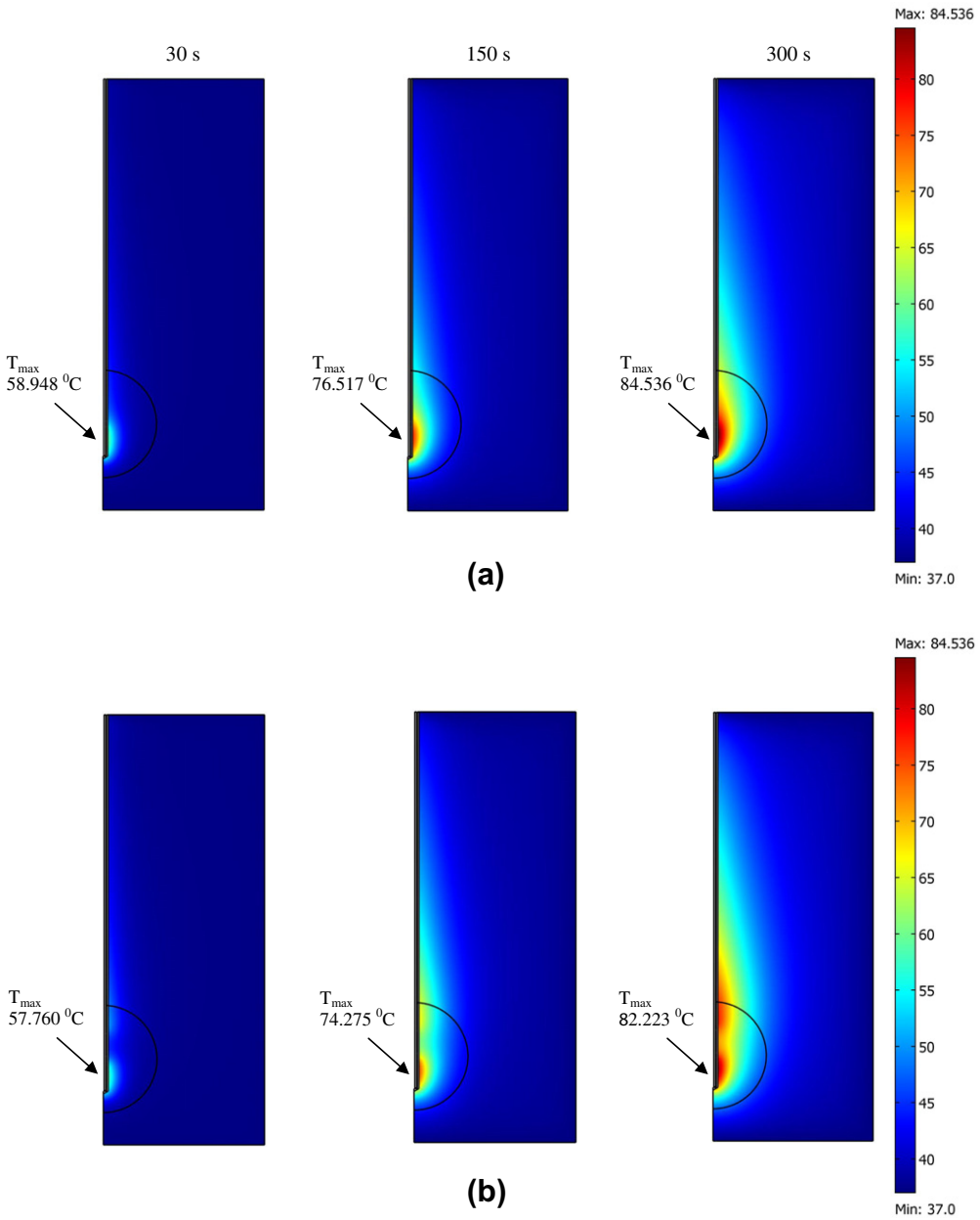

Fig. 10. The temperature profile in the porous liver at various times based on a frequency of 2.45 GHz and input microwave power of 10 W when using; (a) single slot MCA (b) double slot MCA.

z = 16 mm and z = 21.2 mm, respectively. While when using a double slot, the maximum SAR values obtained for 10 W of input microwave power is 2.29 kW/kg and 3.37 kW/kg at z = 16 mm and z = 21.2 mm, respectively. Furthermore, it is seen that when using a single slot MCA generates the SAR distributions at z = 16 mm is higher than at z = 21.2 mm. Nevertheless, the double slot MCA has the SAR distributions at z = 16 mm is lower than at z = 21.2 mm due to the microwave energy through the upper slot before the lower slot. Comparison between maximum SAR values along the extrusion line obtained from the two antennas, it can be seen that the single slot MCA provides a higher maximum SAR value (at z = 16 mm) within the porous liver than that of the double slot MCA (at z = 21.2 mm), which corresponds to a higher SAR profile, as shown in Fig. 8. This is because higher attenuation of the microwave reduces the contributions of propagated waves as they propagate through the double slot MCA. It is found that the variation of SAR distribution within the porous liver is due to the antenna type and the extrusion line position. From the figures, it is found that the variation of the SAR distribution in the porous liver is due to the antenna type and the distance away from the antenna.

5.2.2. Temperature profiles

The effective performance of MWA is characterized by its temperature profile, which is determined mainly using the antenna. In order to simulate the temperature profile as well as heat transfer within the porous liver, the coupled model of transport phenomenon of blood flow, heat transfer and electromagnetic wave propagation are used. The combination of these phenomena has an effect in which the microwave energy can be absorbed by the porous liver and then converted into heat. Fig. 10 shows the simulated results of temperature profile within porous liver at various times based on a same condition as Fig. 8. The temperature profiles within the porous liver when using a single slot MCA and a double slot

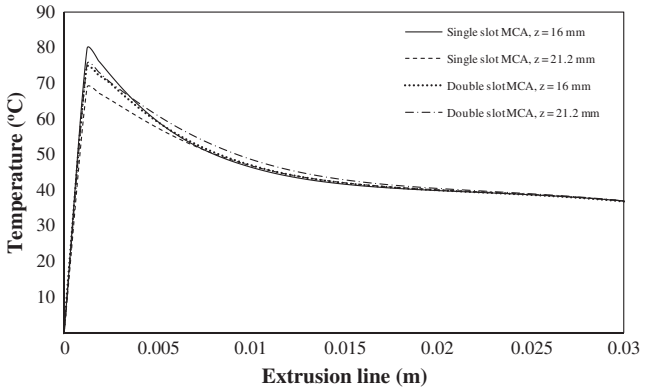

Fig. 11. Comparison of temperature distribution between when using a single slot MCA and a double slot MCA along the extrusion line.

MCA, for heating times of 30, 150, and 300 s, are shown in Fig. 10(a) and (b), respectively. It is observed that the temperature profile within the porous liver corresponds to the SAR profile (Fig. 8). A higher SAR value near the antennas tip and the lower slot exit of the MCA (as shown in Fig. 8) leads to the generation of a hot spot zone in the same location as the SAR. In two cases, the temperature profile forms a nearly ellipsoidal shape around the slot and the highest value occurs in the vicinity of the slot MCA and decreases with the distance following SAR. This is because the SAR within the porous liver distributes, owing to energy absorption. Thereafter, the absorbed energy is converted to thermal energy, lead to increases of temperature in the porous liver. It is found that the maximum temperature within the porous liver of the two cases increases with time. At the early stage of the process (T = 30 s), the heat transfer is manly governed by conduction heat mode. Whereas, in the end stage of the process (T = 300 s), the effect of convective flow increase. This convective effect is especially strong near the tip and the slot of the MCA because it has high temperature volume. The natural convection due to blood flow, are presented in section later. The presences of natural convection heat transfer in the porous liver based on porous media model leads to an infiltrated flow through the tissue pores far away from the MCA as well as hot spot zone. This natural convection effect influences the characteristic of the interaction between microwave and porous liver, which is expected to occur in the realistic physiological condition

Again, corresponding to the SAR pattern, the comparison of the temperature profile pattern between when using a single slot MCA and a using a double slot MCA, illustrates that the volumetric heating within the porous liver of double slot MCA provides the two hot spot zones with a wider region in porous liver around the slot MCA. As opposed to the result when using a single slot MCA which only yields one and narrow region. Furthermore, it is worth to point out that the pattern of the two hot spot zones within the porous liver when using a double slot is not symmetric. That is because the microwave power absorbed within the porous liver attenuates owing to energy absorption, and thereafter the absorbed energy is converted to the thermal energy, lead to increases of temperature in the porous liver.

It is interesting to observe that the temperature profile of the porous liver highest value occurs in the tumor, lead to the temperature of the tumor is higher than the temperature of the normal tissue. In addition, the obtained results show that the maximum temperature calculated from models within the tumor region has temperature higher than 50 °C, which are capable for destroying cancer in the porous liver (Normally, tumor is destroyed at temperatures exceeding 50 °C [1]). Because the double slot MCA provides a wider region in porous liver than the single slot MCA, the normal tissue surrounding the tumor is destroyed more than when using the single slot while considering the tumor diameter of about 20 mm. Therefore, the double slot MCA is suitable for the larger tumor size. By comparison between the maximum temperatures when using a single slot MCA and a double slot MCA, it can be seen that the distribution patterns of temperature at a particular time is the same, but the maximum values are quite different. The single slot MCA provides a higher maximum temperatures value within the porous liver than that of the double slot MCA at all duration times. The maximum temperature differences for the two cases are 2.015% at heating times of 30 s, 2.930% at heating times of 150 s and 2.736% at the heating times of 300 s, respectively. A less than 5% difference between the two cases can be obtained.

With regard to the temperature distribution at the extrusion line (Fig. 7), Fig. 11 shows the comparison of temperature distribution between when using a single slot MCA and a double slot MCA along the extrusion line at level of the upper slot exit and the lower slot exit based on a frequency of 2.45 GHz, input microwave power of 10 W and heating times of 300 s which corresponds to the SAR distribution (Fig. 9). It is seen that the temperature distribution when using a single slot MCA and a double slot MCA have similar trends with a slight difference in magnitude. The temperature quickly increases along the extrusion line to a maximum temperature value at the slot exit. After that the temperature values gradually decreases and approach to steady state. When using a single slot MCA, the maximum temperature values obtained for 10 W of input microwave power is 79.83 and 68.87 °C at z = 16 mm and z = 21.2 mm, respectively. While when using a double slot, the maximum temperature values obtained for 10 W of input microwave power is 74.63 and 75.42 °C at z = 16 mm and z = 21.2 mm, respectively. In addition, it is seen that when using a single slot MCA generate the temperature distributions at z = 16 mm is higher than at z = 21.2 mm. Nevertheless, the double slot MCA has the temperature distributions at z = 16 mm is lower than at z = 21.2 mm following SAR. That is because the microwave power absorbed within the porous liver attenuates owing to energy absorption, and thereafter the absorbed energy is converted to the thermal energy, lead to increases of temperature in the porous liver. The maximum temperature values at level of the upper slot exit (z = 21.2 mm, insertion depth of 58.8 mm) is higher than the maximum temperature values at the lower slot exit (z = 16 mm, insertion depth of 64 mm) when using a double slot due to the microwave energy through the upper slot before the lower slot of this antenna.

When comparison between maximum temperature values along the extrusion line obtained from the two antennas, it can be seen that the single slot MCA provides a higher maximum temperature value (at z = 16 mm) within the porous liver than that of the double slot MCA (at z = 21.2 mm) which corresponds to a higher temperature profile, as shown in Fig. 10. It is found that the antenna type significantly influences to temperatures differences in porous liver.

5.2.3. Blood velocity profiles

The presences of natural convection heat transfer in the porous liver based on porous media model leads to an infiltrated flow through the tissue pores far away from the MCA as well as hot spot zone. This natural convection effect influences the characteristic of the interaction between microwave and porous liver, which is expected to occur in the realistic physiological condition. The effect of natural convection due to the blood flow in the porous liver is presented in Fig. 12. The figure shows the blood velocity profile within the porous liver based on the conditions as mentioned in the previous figures. The blood velocity profile within the porous liver when using a single slot MCA and a double slot MCA, for heating times of 30, 150, and 300 s, are shown in Fig. 12(a) and (b),

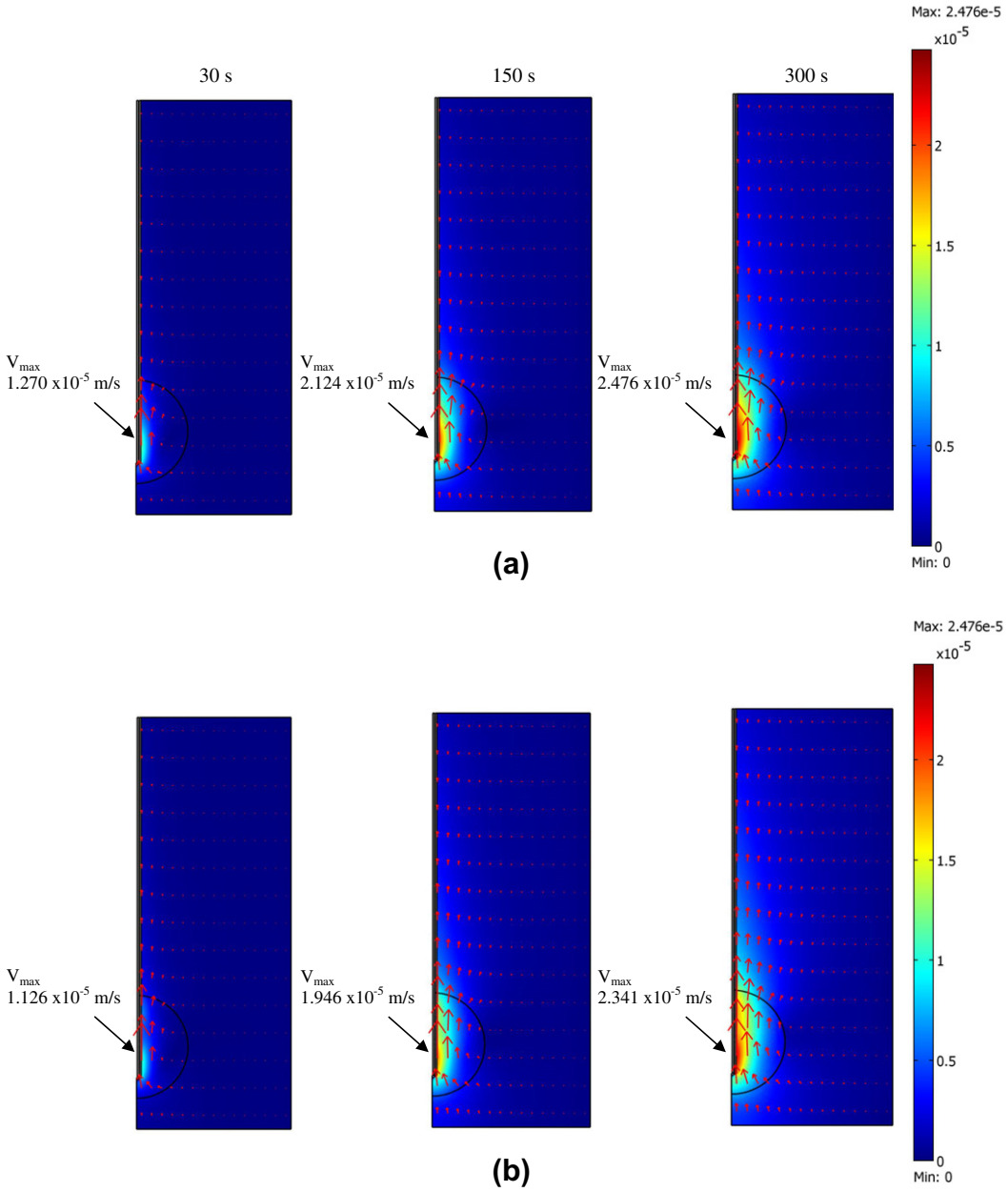

Fig. 12. The blood velocity profile in the porous liver at various times based on a frequency of 2.45 GHz and input microwave power of 10 W when using; (a) single slot MCA (b) double slot MCA.

respectively. The blood velocity profile in two cases have a trend corresponding to the temperature profiles. The blood flow is driven by the effect of buoyancy (natural convection) due to microwave energy. The buoyancy effect is stronger near the tip and the slot of the MCA, leading to a high blood velocity region at location near the tip and the slot of the MCA. The blood velocity profile forms a nearly ellipsoidal shape around the slot corresponding to the temperature profile. Further, it reaches highest values in the vicinity of the slot MCA and decreases with the distance from the single slot MCA axis. The warmer blood with lower density rises near the slot of the MCA, where the surrounding colder blood with higher density displaces the rising warmer blood in the immediate vicinity of the slot MCA. The blood velocity increases rapidly in the early time of heating and reaches a maximum value in a short time. Moreover, the blood velocity within the tumor is higher than the blood velocity within the normal tissue. This is because the tumor has a higher porosity and a higher permeability than normal tissue would lead to stronger microwave energy absorbed as well as natural convection while the normal tissue is of low permeability would leads to the blood velocity within the normal tissue is very weak. It is observed that the blood velocity profiles are varied with corresponding to the temperature profile within the porous liver (Fig. 10). This is because a temperature gradient produced by an electromagnetic field causes a strong effect of natural convection which produces enhanced cooling in porous liver during MWA process. Consider the effect of antenna type on the blood velocity, the double slot MCA provides a slightly lower blood velocity value within the porous liver. This is because the weaknesses of natural convection as compared with using a single slot MCA. It is observed that the maximum blood velocity differences in two cases within the porous liver are decreased with increasing time, during the MWA process. The differences maximum blood velocity value for the two cases

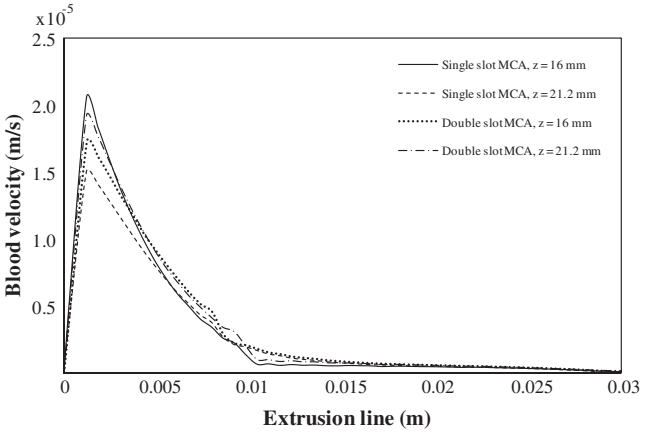

Fig. 13. Comparison of blood velocity distribution between when using a single slot MCA and a double slot MCA along the extrusion line.

are 11.339% at heating times of 30 s, 8.380% at heating times of 150 s and 5.752% at the heating times of 300 s, respectively.

The last section considers the blood velocity distribution at the extrusion line (Fig. 7). Fig. 13 shows the comparison of the blood velocity distribution between when using a single slot MCA and a double slot MCA along the extrusion line at level of the upper slot exit (z = 21.2 mm, insertion depth of 58.8 mm) and the lower slot exit (z = 16 mm, insertion depth of 64 mm) based on a frequency of 2.45 GHz, input microwave power of 10 W and heating times of 300 s which corresponds to the temperature distribution (Fig. 11). It is seen that the blood velocity distribution when using a single slot MCA and a double slot MCA have similar trends with a slight difference in magnitude. The blood velocity quickly increases along the extrusion line to a maximum value at the slot exit and gradually decreases and approach to zero at the outer boundary of the porous liver where no effect of propagating wave occurs. Higher temperature value provides a greater permeability value which leads to a higher blood velocity in the porous liver, thereby increasing the rate of convective heat transfer to keep the porous liver. Therefore, the maximum blood velocity value at z = 16 mm is higher than at z = 21.2 mm when using the single slot MCA and the maximum blood velocity value at z = 16 mm is lower than at z = 21.2 mm when using the double slot MCA following temperature distribution in Fig. 11. Comparison between the maximum blood velocity value obtained from the two antennas, it can be seen that the single slot MCA provides a higher maximum blood velocity value (at z = 16 mm) within the porous liver than that of the double slot MCA (at z = 21.2 mm) which corresponds to a higher blood velocity profile, as shown in Fig. 12.

6. Conclusions

This work presents a numerical study of heat transfer and blood flow coupled with electromagnetic wave propagation in two layers porous liver tissue during MWA process using a single and double slot MCA. The convection heat transfer due to the effect of blood flow is taken into accounts for analysis of heat transfer. The simulation results data of the porous media model (single-layer porous media) is validated against the simulation results of bioheat model obtained from previous work and compared with the experimental results obtained by Yang et al. [20]. The single and double slot MCA for interstitial MWA in porous liver is evaluated in order to compare their effects on the SAR profile, temperature profile and blood velocity profile. It is found that the SAR, temperature and blood velocity value in the porous liver is strongly dependent on the number of MCA slot. The maximum SAR, temperature and blood velocity appears in the porous liver when using a single slot MCA which is higher than when using a double slot antenna. It is found that the SAR, temperature and blood velocity pattern when using a double slot MCA provides a wider region in porous liver around the slot MCA and has two hot spot zones which occurs in the vicinity of these double slots. Consequently, the single slot MCA is generally suitable for the narrow tumor while, the double slot MCA is suitable for the larger tumor size or adjacent tumors. In addition, the shape and size of the destructed area can be varied by adjusting the configuration and antenna design, resulting in no damage to the normal tissues. Although, the blood velocity in this problem is very small as compared to the conventional problem in the literatures. Less than a ten percent difference between the two cases in blood velocity value can be obtained. However, the main idea behind this work is to propose the completed model, i.e., multilayer porous media model in order to completely explain the actual process of MWA within the liver. Conclusively, the mathematical model presented in this study correctly explains the phenomena of heat transfer and blood flow in porous liver tissue during MWA process using a single and double slot MCA.

In next step of this research, will to develop a three-dimensional modeling for approaching realistic liver tissue will be performed. The study will also consider local non-thermal equilibrium (LNTE) heat transfer model in analyzing biological tissues subjected to microwave energy.

Acknowledgments

This work was financially supported by the National Research University Project of Thailand Office of Higher Education Commission and the Thailand Research Fund (TRF) under the Royal Golden Jubilee Ph.D. Program (RGJ) Contract No. PHD/0362/2551 and Thammasat University.

References

[1] J.P. McGahan, J.M. Brock, H. Tesluk, W.Z. Gu, P. Schneider, P.D. Browing, Hepatic ablation with use of radio-frequency electrocautery in the animal model, J. Vasc. Intervent.l Radiol. JVIR 3 (2) (1992) 291–297.
[2] S. Garrean, J. Hering, A. Saied, P.J. Hoopes, W.S. Helton, T.P. Ryan, N.J. Espat, Ultrasound monitoring of a novel microwave ablation (MWA) device in porcine liver: lessons learned and phenomena observed on ablative effects near major intrahepatic vessels, J. Gastrointest. Surg. 13 (2) (2009) 334–340.
[3] T. Seki, M. Wakabayashi, T. Nakagawa, M. Imamura, T. Tamai, A. Nishimura, N. Yamashiki, et al., Percutaneous microwave coagulation therapy for patients with small hepatocellular carcinoma: comparison with percutaneous ethanol injection therapy, Cancer 85 (8) (1999) 1694–1702.
[4] L. Solbiati, T. Livraghi, S.N. Goldberg, T. Ierace, F. Meloni, M. Dellanoce, L. Cova, et al., Percutaneous radio-frequency ablation of hepatic metastases from colorectal cancer: long-term results in 117 patients, Radiology 221 (1) (2001) 159–166.
[5] K. Saito, H. Yoshimura, K. Ito, Y. Aoyagi, H. Horita, Clinical trials of interstitial microwave hyperthermia by use of coaxial-slot antenna with two slots, IEEE Trans. Microw. Theory Tech. 52 (8 II) (2004) 1987–1991.
[6] P. Keangin, T. Wessapan, P. Rattanadecho, Analysis of heat transfer in deformed liver cancer modeling treated using a microwave coaxial antenna, Appl. Therm. Eng. 31 (16) (2011) 3243–3254.
[7] Deshan Yang, J.M. Bertram, M.C. Converse, A.P. O'Rourke, J.G. Webster, S.C. Hagness, J.A. Will, D.M. Mahvi, A floating sleeve antenna yields localized hepatic microwave ablation, IEEE Trans. Biomed. Eng. 53 (3) (2006) 533–537.
[8] C.L. Brace, D.W. Van Der Weide, F.T. Lee Jr., P.F. Laeseke, L. Sampson, Analysis and experimental validation of a triaxial antenna for microwave tumor ablation, in: IEEE MTT-S International Microwave Symposium Digest, vol. 3, 2004, pp. 1437–1440.
[9] C.L. Brace, P.F. Laeseke, L.A. Sampson, T.M. Frey, D.W. Van Der Weide, F.T. Lee Jr., Microwave ablation with multiple simultaneously powered small-gauge triaxial antennas: results from an in vivo swine liver model, Radiology 244 (1) 151–156.
[10] Y. Sun, Z. Cheng, L. Dong, G. Zhang, Y. Wang, P. Liang, Comparison of temperature curve and ablation zone between 915- and 2450-MHz cooled-shaft microwave antenna: results in ex vivo porcine livers, Eur. J. Radiol. 81 (3) (2012) 553–557.
[11] Q. Zhou, X. Jin, D.-C. Jiao, F.-J. Zhang, L. Zhang, X.-W. Han, G.-F. Duan, et al., Microwave ablation results in ex vivo and in vivo porcine livers with 2450-MHz cooled-shaft antenna 124 (20) (2011) 3386–3393.

[12] L. Hadizafar, M.N. Azarmanesh, M. Ojaroudi, Enhanced bandwidth double-fed microstrip slot antenna with a pair of L-shaped slots, Prog. Electromagnet. Res. 18 (2011) 47–57.
[13] L. Li, W. Che, Y. Chang, Investigations on an improved interstitial antenna used for microwave hyperthermia and the specific absorption rate distribution within biological tissues, Microw. Optical Technol. Lett. 54 (2) (2012) 405–409.
[14] T. Terakawa, K. Ito, K. Ueno, M. Hyodo, H. Kasai, Design of interstitial ring-slot applicator for microwave hyperthermia, in: IEEE Engineering in Medicine and Biology Society 11th Annual International Conference, 1989, pp. 1147.
[15] M.F.J.C. Rubio, A.V. Hernández, L.L. Salas, E. Ávila-Navarro, E.A. Navarro, Coaxial slot antenna design for microwave hyperthermia using finite-difference time-domain and finite element method, Open Nanomed. J. 3 (2011) 2–9.
[16] M. Hyodo, M. Shimura, K. Ito, H. Kasai, Basic study on interstitial applicators with a single ring slot for microwave hyperthermia, in: IEEE Engineering in Medicine and Biology Society Annual International Conference, vol. 12, issue 4, 1990, pp. 1555.
[17] S. Park, Y. Lim, Antenna design for catheter-based tissue heating, in: IEEE International Conference on Computational Electromagnetics and Its Applications Proceedings 3rd, 2004, pp. 189–192.
[18] A.U. Hines-Peralta, N. Pirani, P. Clegg, N. Cronin, T.P. Ryan, Z. Liu, S.N. Goldberg, Microwave ablation: results with a 2.45-GHz applicator in ex vivo bovine and in vivo porcine liver, Radiology 239 (1) (2006) 94–102.
[19] H.H. Pennes, Analysis of tissue and arterial blood temperatures in the resting human forearm, J. Appl. Physiol. 85 (1) (1998) 5–34.
[20] D. Yang, M. Converse, D. Mahvi, Expanding the bioheat equation to include tissue internal water evaporation during heating, IEEE Trans. Biomed. Eng. 54 (8) (2007) 1382–1388.
[21] Ş. Özen, S. Helhel, O. Çerezci, Heat analysis of biological tissue exposed to microwave by using thermal wave model of bio-heat transfer (TWMBT), Burns 34 (1) (2008) 45–49.
[22] P. Keangin, P. Rattanadecho, T. Wessapan, An analysis of heat transfer in liver tissue during microwave ablation using single and double slot antenna, Int. Commun. Heat Mass Transfer 38 (6) (2011) 757–766.
[23] K. Khanafer, K. Vafai, The role of porous media in biomedical engineering as related to magnetic resonance imaging and drug delivery, Transfer/Waerme- und Stoffuebertragung 42 (10) (2006) 939–953.
[24] A. Nakayama, F. Kuwahara, A general bioheat transfer model based on the theory of porous media, Int. J. Heat Mass Transfer 51 (2008) 3190–3199.
[25] S. Mahjoob, K. Vafai, Analytical characterization of heat transport through biological media incorporating hyperthermia treatment, Int. J. Heat Mass Transfer 52 (5–6) (2009) 1608–1618.
[26] N. Afrin, Y. Zhang, J.K. Chen, Thermal lagging in living biological tissue based on nonequilibrium heat transfer between tissue, arterial and venous bloods, Int. J. Heat Mass Transfer 54 (11–12) (2011) 2419–2426.
[27] K. Saito, Y. Hayashi, H. Yoshimura, K. Ito, Heating characteristics of array applicator composed of two coaxial-slot antennas for microwave coagulation therapy, IEEE Trans. Microw. Theory Technol. 48 (2000) 1800–1806 (1 PART 1).
[28] J.M. Bertram, D. Yang, M.C. Converse, Antenna design for microwave hepatic ablation using an axisymmetric electromagnetic model, Biomed. Eng. Online 5 (2006).
[29] R.D. Nevels, G.D. Arndt, G.W. Raffoul, J.R. Carl, A. Pacifico, Microwave catheter design, IEEE Trans. Biomed.l Eng. 45 (1998) 885–900.
[30] T. Wessapan, S. Srisawatdhisukul, P. Rattanadecho, The effects of dielectric shield on specific absorption rate and heat transfer in the human body exposed to leakage microwave energy, Int. Commun. Heat Mass Transfer 38 (2) (2011) 255–262.
[31] Z.P. Chen, W.H. Miller, R.B. Roemer, T.C. Cetas, Errors between two- and three-dimensional thermal model predictions of hyperthermia treatments, Int. J. Hyperth. 6 (1) (1990) 175–191.
[32] P.R. Stauffer, F. Rossetto, M. Prakash, D.G. Neuman, T. Lee, Phantom and animal tissues for modeling the electrical properties of human liver, Int. J. Hyperth. 19 (1) (2003) 89–101.
[33] M. Cepeda, A. Vera, L. Leija, C. Trujillo, Coaxial double slot antenna design for interstitial hyperthermia in muscle using a finite element computer modeling, in: IEEE International Instrumentation and Measurement Technology Conference I2MTC, 2008, pp. 961–963.
[34] J. Fan, L. Wang, A general bioheat model at macroscale, Int. J. Heat Mass Transfer 54 (1–3) (2011) 722–726.
[35] D. Poulikakos, K. Renken, Forced convection in a channel filled with porous medium, including the effects of flow inertia, variable porosity, and Brinkman friction, J. Heat Transfer 109 (4) (1987) 880–888.
[36] M.L. Hunt, C.L. Tien, Effects of thermal dispersion on forced convection in fibrous media, Int. J. Heat Mass Transfer 31 (2) (1988) 301–309.
[37] H.C. Brinkmann, On the permeability of media consisting of closely packed porous particles, Appl. Sci. Res. 1 (1947) 81–86.
[38] W. Klinbun, P. Rattanadecho, W. Pakdee, Microwave heating of saturated packed bed using a rectangular waveguide (TE10 mode): influence of particle size, sample dimension, frequency, and placement inside the guide, Int. J. Heat Mass Transfer 54 (2011) 1763–1774.
[39] K. Vafai, Convective flow and heat transfer in variable porosity media, J. Fluid Mech. 147 (1984) 233–259.
[40] D.A. Nield, A. Bejan, Convection in Porous Media, second ed., Springer-Verlag, Inc., New York, 1999.
[41] A.M. Al-Amiri, Analysis of momentum and energy transfer in a lid-driven cavity filled with a porous medium, Int. J. Heat Mass Transfer 43 (19) (2000) 3513–3527.